JOURNAL OF SPACECRAFT AND ROCKETS
Vol. , No. ,

Survivability Evaluation of Electrodynamic Tethers Considering Dynamic Fracture in Space-Debris Impact

Kanjuro Makihara* and Ryo Takahashi†
Tohoku University, Sendai 980-8579, Japan

DOI: 10.2514/1.A33328

1 **Electrodynamic tethers are used to remove large uncontrollable satellites from low Earth orbits. However, tether**
2 **systems are vulnerable to collisions with space debris orbiting at high speeds. Such collisions can easily sever**
3 **electrodynamic tethers. The success of an electrodynamic tether mission to remove uncontrollable satellites from low Earth orbits will depend in part on how often the electrodynamic tether collides with space debris and how the electrodynamic tether fractures as a result of a collision. The dynamic fracture progress of an electrodynamic tether in response to a collision with space debris has not been previously considered in predicting the success rate of an electrodynamic tether mission. In this study, the fracture progress of an electrodynamic tether owing to a hypervelocity impact collision with space debris was experimentally and numerically examined to understand the dynamic fracture phenomenon. In addition, an estimate of the survivability of an electrodynamic tether in orbit was made, which included a consideration of the dynamic fracture of the tether, and this estimate was found to be lower than the survivability estimate, which did not consider the dynamic fracture of the tether.**

Nomenclature

$A(d)$	=	effective cross-sectional area as a function of d, without considering dynamic fracture
$A_\alpha(d)$	=	effective cross-sectional area as a function of d, by considering dynamic fracture
D_T	=	diameter of tether
D_{TC}	=	critical distance of tether (minimum distance of tether to survive)
d	=	diameter of space debris particle
d_m	=	minimum diameter of space debris particle to sever a tether
L_T	=	length of tether
R	=	fatal impact rate (number of debris collisions per year)
R_T	=	residual distance of tether after collision
t	=	time, year
$X(t)$	=	survivability of tether at time t
x	=	overlapped distance between debris and tether
α	=	progress distance of dynamic fracture
γ	=	ratio of α to x
$\varphi(d)$	=	debris flux (number of debris particles per year per square meter) as a function of d

I. Introduction

THE promotion of space development in the future requires that space debris should not be neglected. Space debris consists of defunct manmade objects in the space environment. These objects are a major threat to space development [1,2]. Space debris travels at very high velocities and can cause extensive damage to currently operated satellites or the International Space Station. Therefore, for future space development, it is important to reduce the amount of space debris. Of the various types of space debris that exist, large uncontrollable satellites are the highest-priority objects that need to be removed from orbit because they possess the greatest potential to generate large amounts of debris when they break apart or collide with smaller pieces of space debris.

Electrodynamic tethers (EDTs) have been proposed for use in removing uncontrollable satellites from low Earth orbits (LEOs) [3–8]. Figure 1 shows the principle of operation of an EDT. Although the basic concept of EDTs and the procedure for removal of space debris using EDTs have been described in the literature [3,9–11], a brief explanation is offered here so that the reader may better understand what follows. An EDT consists of a conductive tether, an emitter, and a collector. After the conductive tether is attached to a target satellite, the collector starts to collect electrons, and the emitter starts to emit electrons. Because of the motion of the electrons, electric current flows in the longitudinal direction of the conductive tether. A pseudocircuit can be created with the conductive tether and the space atmosphere by collecting electrons from plasma in the space environment at one end and emitting electrons at the other end. A Lorentz force is induced in the tether by the interference between the current flow and the geomagnetic field. This force can decelerate the traveling speed of the target satellite because the force acts in the direction opposite to the traveling direction of the target. The slower velocity of the satellite breaks the equilibrium between centrifugal and gravitational forces, and eventually the satellite deviates from its orbit and falls to the Earth. Because an EDT does not require any propellant to deorbit a target satellite, the total mass of the EDT can be much less than that of a conventional rocket-based deorbit system. The light weight of EDT systems is a great advantage over conventional space debris removal systems. The mathematics of the complex motion dynamics of EDTs have been studied extensively [12–15]. The tethers used are thin but long enough to have sufficiently large surface areas that they are subject to collisions with small pieces of space debris. Accidental collisions with space debris can easily sever the tethers. The success of an EDT mission to remove uncontrollable satellites from LEOs depends greatly on the survivability of the tether (i.e., the probability of being not severed during the mission). Therefore, it is necessary to accurately estimate the survival probability of the tether to predict the survivability of an EDT mission.

II. Problem Statement and Research Objectives

Previous studies on the survival probability of EDTs [16–19] have one or more of the following three limitations to their success in estimating hypervelocity impact fracture. First, the fracture of an EDT tether after debris impact has not been clearly defined. The lack of a standard definition for impact fracture has led to a range of results in the fracture evaluation of tethers. The definition of the critical distance [8,19] of a tether, which is required for the tether to survive a

Received 21 April 2015; revision received 2 September 2015; accepted for publication 28 September 2015; published online XX epubMonth XXXX.

*Associate Professor, Department of Aerospace Engineering, 6-6-01 Aramaki-Aza-Aoba, Aoba-Ward; makihara@ssl.mech.tohoku.ac.jp. Member AIAA.

†Student, Department of Aerospace Engineering, 6-6-01 Aramaki-Aza-Aoba, Aoba-Ward.

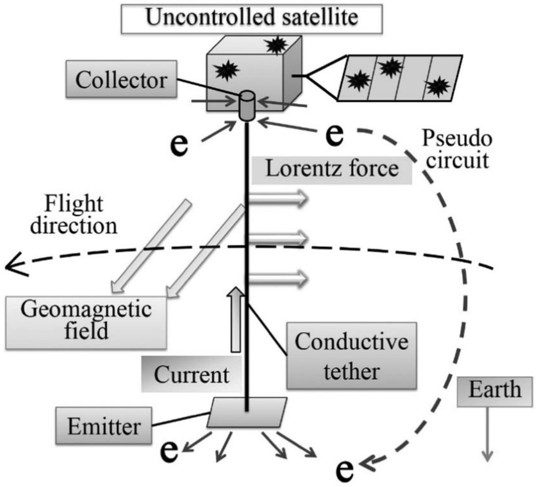

Fig. 1 Principle of electrodynamic tether.

debris impact, has been a particularly controversial subject. Several studies have made particular mention of the critical distance. The area of the fracture of tethers after the impact is essential to evaluate the damage of tethers. One study assumed that the fracture area of the tether coincides with the path of the debris [17]. This assumption is too simple when considering the actual fracture after the impact because there is a chance that, as a result of the hypervelocity collision, the fracture of the tether will progress from the path. In other words, the fracture of the tether may be larger than the path area. Another assumption made in previous research is that the fracture of the tether is three times greater than the debris diameter [20]. This assumption is derived from the empirical results of experiments of hypervelocity impacts against a thick metal that were conducted by Simon et al. [21]. The target metal has large thickness and creates a crater rather than a penetration hole. However, because the collision configuration of a thin tether is completely different from that of a thick metal, the empirical coefficient number (i.e., 3) for the fracture based on impact experiments in that study might not be valid in impact experiments for tethers. To address this limitation, we introduce a factor of safety (FS) and define the critical distance of the tether in a more rigorous way.

The second limitation of previous studies is that the fracture of the tether after impact has not been investigated experimentally, although many impact experiments involving bumper shields ([22], for example) have been conducted. Some studies on tether systems were conducted experimentally. Hörtz et al. [23] made experiments of impacts on aluminum foil of decreasing thickness, which showed that the transition from craters to penetration holes. Sabath and Paul [24] carried out hypervelocity impact experiments on nonconductive tether materials. They reports observations of hypervelocity impact experiments on three different braided materials used for tether applications. Francesconi et al. [25] conducted impact experiments and evaluated the impact damage of tape tethers. Their experiments showed that the impact damage is very close to the projectile size in case of normal impact, whereas it increases significantly at highly oblique impact angles. However, the number of the experiments of tether systems is much fewer than that of bumper shields. In this study, we carried out hypervelocity impact experiments on tether systems using large-scale experimental equipment.

The third limitation is that it is difficult to measure the path of space debris in hypervelocity impact experiments. The path must be measured to estimate the actual fracture. We therefore devised a new method to measure the path of the debris experimentally. The fracture of the tether can be determined from the measured path of the debris.

In this study, we analyzed the fracture of the tether due to collision with space debris. We carried out numerical simulations of the collision impact between a tether and space debris and gained new insights into the phenomenon of tether fracture due to hypervelocity impact. Hypervelocity impact experiments were carried out using a high-explosive gun as the impact instrument to validate the simulation results. We devised a new experimental method to determine the trajectory of the debris. The insight gained into the phenomenon of tether fracture due to hypervelocity impact led to a new approach to tether fracture evaluation. By taking into consideration this fracture phenomenon and using a debris flux model provided by NASA, we were able to develop a new method for estimating the survivability of an EDT in orbit.

III. Numerical Simulation

A. Smoothed Particle Hydrodynamics

We analyzed the phenomenon of tether fracture in collision with small-sized debris using numerical simulation based on the smoothed particle hydrodynamics (SPH) method [26]. The SPH simulation method involves dividing the analyzed object into particles and following the motion of each particle, in a manner similar to that of the Lagrange method. The SPH method does not require any computational grids, which is one of its major advantages over conventional computation methods. This method yields the physical quantity at any spot in the calculation area by compensating for the physical quantity of particles around the spot. The SPH method is often used in numerical simulation of hypervelocity impacts and large-scale fracture phenomena. This method is regarded as being suitable for simulating hypervelocity impacts and dynamic fracture after impact.

Figure 2 shows the simulation model of the collision between the tether and the space debris and indicates their initial positions. We assumed that the tether was cylindrical in shape and that the space debris was spherical in shape. The diameter of the tether was 1 mm, and that of the debris was also 1 mm. The impact velocity was 6.0 km/s. In the simulation, the debris collides with the tether while moving downward, as shown in the figure. The overlapped distance between the debris and the tether is described by x in the initial position. Figure 3 shows the cross section of the tether after the debris collision. The shaded area to the right represents the travel path of the debris. The residual area of the tether is represented by the crescent shape to the left in Fig. 3. Between the residual tether and the debris path, there is nothing left (as indicated by the hatched area in Fig. 3). This half-moon shaped area is shaved off by the debris impact. Apparently, the fracture area progresses from the boundary of the debris path. Thus, we concluded that the assumption made in a previous study [17] that the fracture area of the tether was the same as that of the debris path was invalid. We obtained details of the fracture produced by the collision between the tether and the debris from the measurements illustrated in Fig. 3. The diameter of the tether before the collision is D_T, and the residual distance along the center line (the thickest distance of the residual tether) after the collision is R_T. The subscript T denotes the tether. The path of the debris completely removes the tether, and nothing remains. Furthermore, because of the hypervelocity collision, the fracture area of the tether progresses from the path area. In other words, the fracture area of the tether is larger than the collision area. Note that the fracture after the impact has to be

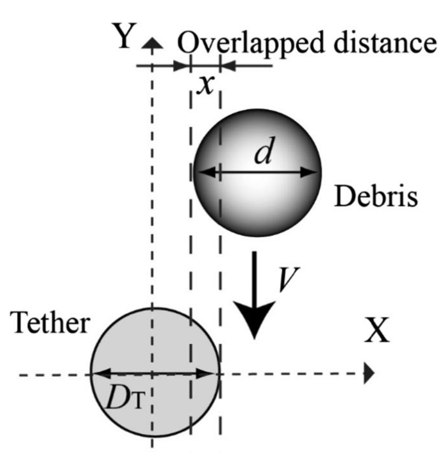

Fig. 2 Initial positions of debris and tether before collision in numerical simulation model.

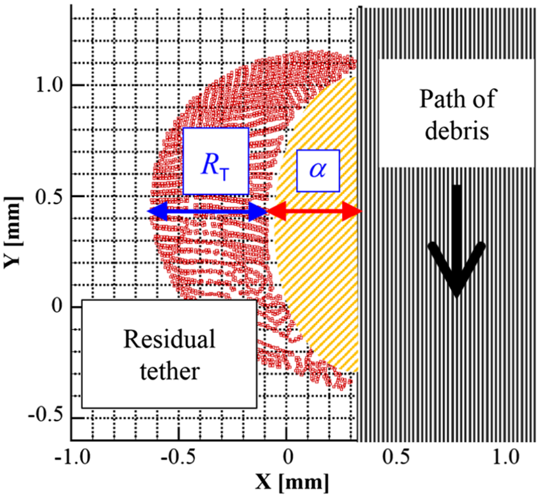

Fig. 3 Cross section of tether after collision ($V = 6.0$ km/s and $d = 1$ mm).

considered to evaluate the fracture at impact. This additional fracture is referred to as dynamic fracture in this paper because it occurs just after the impact. We refer to the area in which the dynamic fracture progresses after collision as the distance of fracture progress, denoted by α in Fig. 3. The hypervelocity collision induces high temperatures and stress in the tether and thereby induces the dynamic progress of the fracture. This paper focuses on the macroscopic influence of the fracture on the tether mission rather than the microscopic causal investigation of fracture phenomenon.

B. Analysis of Residual Distance of Tether

We analyzed the residual distance of the tether after the debris collision using SPH simulation. The critical distance of the tether after the impact, D_{TC}, is the criterion for whether the tether is severed or not. When the residual distance of the tether equals the critical distance (i.e., $R_T = D_{\mathrm{TC}}$), the tether is completely severed. There have been several studies on the critical distance of the tether. Cosmo and Lorenzini [3] touched upon the issue of the critical distance and wrote that D_{TC} is $0.7D_T$. This assumption suggests that the tether could be severed when the debris grazes the critical distance of the tether. The value of the coefficient is based on a tentative assumption, and it was adopted in Action Item 19.1 tests managed by Inter-Agency Space Debris Coordination Committee [27,28]. Anselmo and Pardini [6] and Pardini et al. [8,18,19] estimated the survivability of EDTs based on this assumption [3]. It is important to note that each of these studies has relied on an assumption concerning the critical value of tether diameter, D_{TC}, and we also note that a widely accepted definition of the critical distance has not been established. As mentioned previously, some studies have implied that the critical value seems to include the fracture progress α, whereas others have implied that the critical value does not include the fracture progress. Furthermore, the actual tether diameter is not always linked to its critical distance because a sufficient safety margin is determined in the design stage for the EDT mission and the tether structure.

We clarify the definition of D_{TC} and D_T by introducing a factor of safety (FS) value. The FS is a term describing the structural capacity of a system beyond the expected impacts or loads, which can lead to the reliability of a design. The FS value can provide solid evidence for designing the diameter of the tether, which can be accepted as a commonly recognized value. The FS value stipulates enough margin of the tether to survive the debris collision. When we design an EDT system, we first have to determine the value of D_{TC}. The value is determined with the value of the maximum tension of the tether, Lorentz force, descending acceleration, yield stress, mass of a target satellite, and so forth. The maximum tension of the tether is determined during the design of an EDT mission to remove a target satellite. The Lorentz force is determined from the geomagnetic field and the drive capabilities of the emitter and the collector. We next have to determine the value of D_T using a prescribed FS value, which is usually stipulated by design engineers. The diameter of the tether is related to the critical distance as follows:

$$D_{\mathrm{T}} = \mathrm{FS} \times D_{\mathrm{TC}} \tag{1}$$

The FS value can provide solid evidence for designing the diameter of the tether, which can be accepted as a commonly recognized value. The FS value commonly used in aerospace engineering ranges from 1.15 to 1.5. In this study, we set the FS value to 1.5.

Figure 4 shows the simulation results for the residual distance of the tether for debris diameters of 0.33, 0.67, and 1.0 mm. The overlapped distance between the tether and the debris at the initial position as shown in Fig. 2 is plotted on the horizontal axis. The residual distance of the tether after collision, R_T, is plotted on the vertical axis. The diameter of the tether, D_T, was 1.0 mm in this simulation. From Eq. (1), the critical distance is 0.67 mm. Therefore, the tether will be severed when the residual distance R_T becomes less than 0.67 mm. As seen in Fig. 4, the tether is always severed by the collision with the debris, regardless of the debris diameter, when the overlapped distance is greater than 0.08 mm. In this case, the distance of the dynamic fracture progress α, defined in Fig. 3, is measured as $\alpha = 0.25D_T$. The overlapped distance is $0.08D_T$ when $\alpha = 0.25D_T$. When we introduce the relationship $\alpha = \gamma x$, we obtain $\gamma = 0.25D_T/0.08D_T$.

We also conducted simulations for another tether configuration. Figure 5 shows the simulation results for debris diameters of 3.3, 6.7, and 10.0 mm. The diameter of the tether in these cases was 10 mm. In these cases, the tether was severed when the overlapped distance was greater than 0.9 mm. The progress distance of dynamic fracture, α, was calculated as $\alpha = 0.24D_T$. Therefore, in both sets of cases, the fracture area that included the dynamic fracture area was greater than

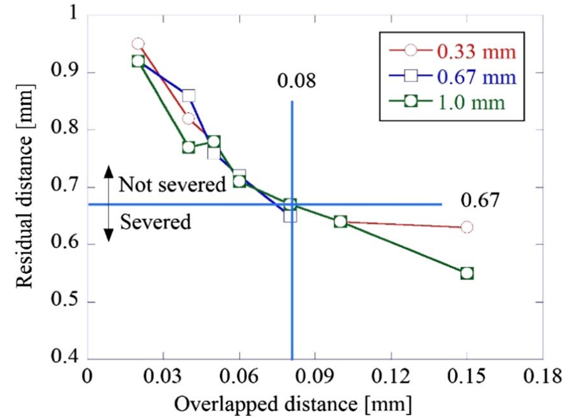

Fig. 4 Residual distance of tether (diameter of tether is 1.0 mm).

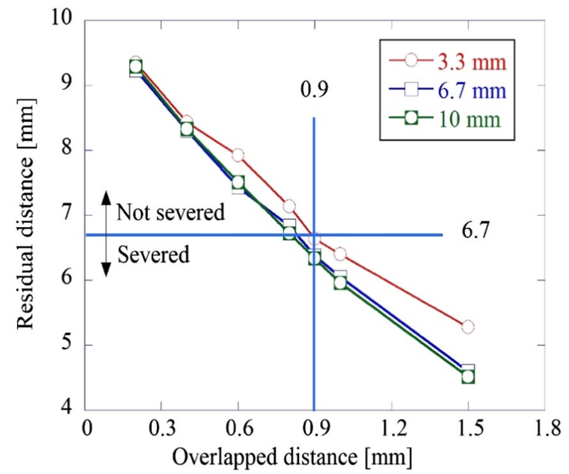

Fig. 5 Residual distance of tether (diameter of tether is 10 mm).

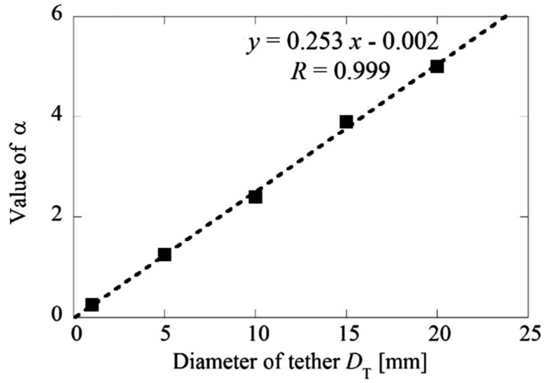

Fig. 6 Fracture progress α for diameter of tether D_T.

Fig. 7 High-explosive gun (Institute of Fluid Science, Tohoku University).

the area of the debris path, and the values of α/D_T for the two sets of cases were essentially the same. When $\alpha = 0.24D_T$, the overlapped distance is $0.09D_T$ and $\gamma = 0.24D_T/0.09D_T$.

Simulations were also conducted for a range of tether diameters. We calculated values of α for the five tether diameters shown in Fig. 6. The slope of the regression line (i.e., the value of α/D_T) remains almost constant at 0.253, regardless of the diameter of the tether. The correlation coefficient of the regression line is 0.999, which indicates that the regression equation fits the data very well. In other words, α/D_T is independent of the size of the tether. Therefore, it is possible to estimate the value of α, regardless of the diameter of the tether, which means that the shape of the dynamic fracture remains similar for any size of the tether. The progress distance of dynamic fracture, α, can be quantitatively determined for fracture of tethers in collision with the space debris. The average value of γ is $0.253D_T/0.085D_T = 2.98$ because the average value of the overlapped distance is $0.085D_T$ for all calculation cases.

IV. Hypervelocity Impact Experiments

A. Experimental Outline

To investigate the nature of the dynamic fracture of the tether, we conducted hypervelocity impact experiments with the high-explosive gun [29] located at the Institute of Fluid Science of Tohoku University, shown in Fig. 7. Figure 8 is a diagram of the one-stage high-explosive gun, which consists of a pump tube 51 mm in diameter and 3400 mm in length, a launch tube 15 mm in diameter and 3000 mm in length, and a recovery chamber 12 m in length with an inner diameter of 1.7 m. The gun is made of stainless steel and has three observation sections 600 mm in diameter with 20-mm-thick acrylic windows. The recovery chamber was evacuated using a turbomolecular pump that can reduce the internal pressure to less than 1 Pa.

There have only been a few reports of experiments on tether impacts. These experiments have involved the use of quite thin aluminum wires, 0.4 mm in diameter, as tethers [30]. Because tiny debris particles were shot at tethers (0.4 mm in diameter) in these experiments, it was difficult to distinguish between the path areas of the debris and the fracture areas of the tethers in these experiments. To resolve this difficulty, we invented a new method to distinguish between the fracture area and the path area. As Fig. 9 shows, two aluminum bars were used. The method that we devised to identify the debris path was to shoot the debris so that the debris would graze the left end of the right aluminum bar. The direction of the debris particles was gradually adjusted to touch the target bar by trial and error. We were thereby able to distinguish between the debris path and the fracture area. The bars had diameters of 10 mm. The distance between the two aluminum bars was 22.5 mm. The projectile that was shot as space debris was a cylinder of polycarbonate 15 mm in diameter and 15 mm in height. These experimental parameters are summarized in Table 1.

B. Results of Impact Experiments

Figure 10 shows the results of the impact experiments. The left bar was the target tether and was bent by the impact shock, which was not the focus of this study. The right bar served as a guide to provide a contact point to trace the debris path. We confirmed that the projectile grazed the right bar, which was our intention with the experimental configuration shown in Fig. 9. The fracture of the left aluminum bar progressed in the same way as in the SPH simulation (Fig. 3). The

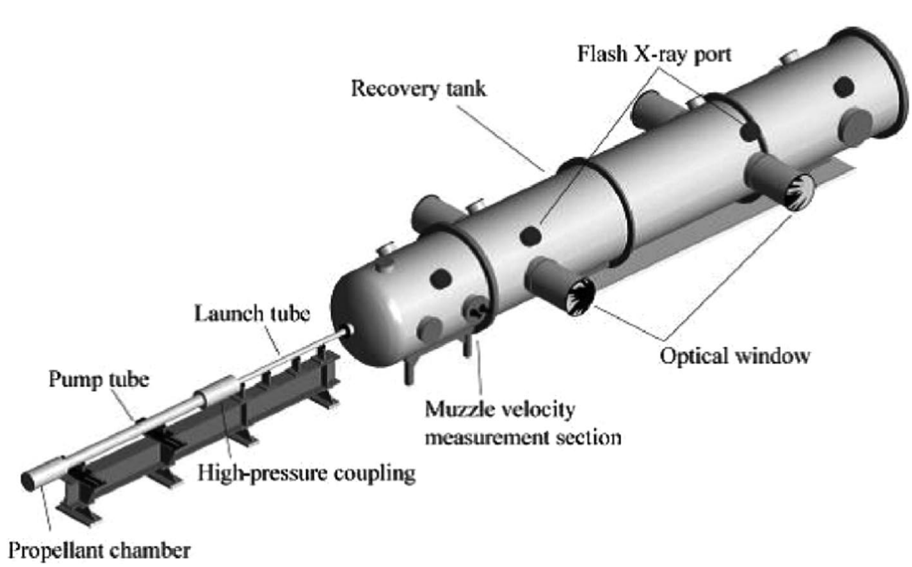

Fig. 8 Illustration of high-explosive gun used in hypervelocity impact experiment.

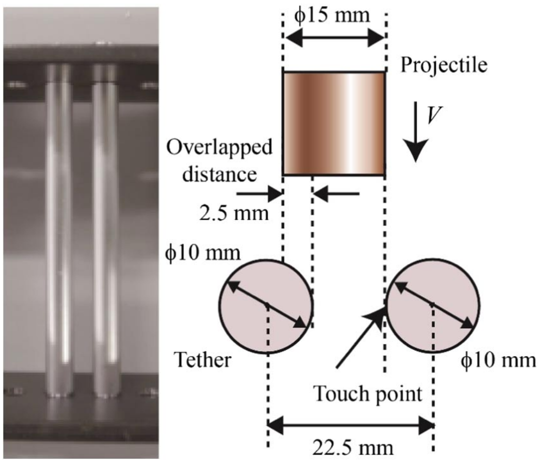

Fig. 9 Target bars for impact experiments (left end of right bar is touch point).

residual distance of the aluminum bar, R_T, was 5.3 mm. The progress distance $D_T - R_T$ was 4.7 mm (equal to $10.0 - 5.3$). The overlapped area was 2.5 mm. Therefore, it is clear that the fracture area (4.7 mm) was larger than the overlapped distance (2.5 mm). These results are consistent with those of the SPH simulation.

Table 2 shows a comparison between the results obtained in the impact experiment and the SPH simulation. The results were obtained for the same hypervelocity impact conditions. The results of the experiment agreed very well with those of the SPH simulation in terms of the residual distance after the collision. The simulation result and experimental result differed by only 1.9%, which confirms the validity of our fracture model for hypervelocity impact. Because the SPH simulation is two-dimensional, the center area (A-A' in Fig. 10) is practically important, and the edges are insignificant, despite the discrepancy between the results shown in Figs. 3, 10.

5

V. Improved Probability Formulation of Electrodynamic Tether by Considering Dynamic Fracture

In this section, we improve the survival probability formulation of EDT systems, considering the dynamic fracture that we have discussed. The survivability calculation approach described later is consistent with that used in previous studies [8,17–19]. EDT systems have been proposed to remove large uncontrollable satellites from orbit by flowing electric current through the conductive tether and generating electrodynamic forces, which cause them to deorbit. During such removal missions, small space debris can accidentally collide with the EDT tether. If the tether is severed, an EDT mission to remove large satellites will fail. An EDT system moves large uncontrollable satellites from the orbit and fall to the Earth by flowing electric current through the conductive tether. During the removal mission, the small space debris accidentally collides with the EDT tether. If the tether is severed, the EDT mission to remove large satellites fails. As shown in Fig. 11, a tether can be severed by space debris with a diameter of d when the debris edge passes within a critical distance $\pm D_{\mathrm{TC}}/2$ from the longitudinal axis of symmetry of the tether. In other words, the tether can be severed when the center of the debris passes an area within $\pm(D_{\mathrm{TC}}/2 + d/2)$ from the longitudinal axis of the tether. Thus, the conventional effective cross-sectional area for severance of the tether in previous studies [8,17–19] is obtained as follows:

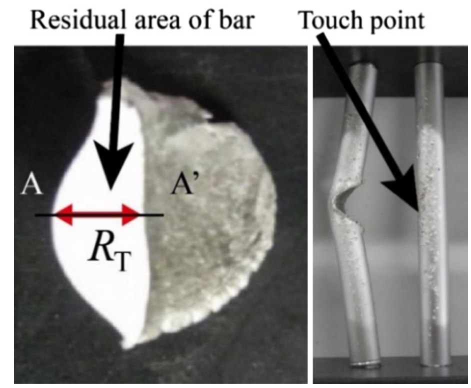

Fig. 10 Aluminum bars after impact.

$$A(d) \equiv L_T(D_{\mathrm{TC}} + d) \tag{2}$$

The tether will be severed when the center of the space debris travels within the effective area $A(d)$. This conventional effective cross-sectional area was used for single and double tethers [8,17–19], but the distance of the fracture progress after the debris collision, α, was ignored in these studies. This approach to estimating the survivability of the tether has also been applied to other types of tethers, such as tape tethers [20,31].

In contrast to the conventional definition of the cross-sectional area, our definition of the effective cross-sectional area accounts for the fracture progress α, shown in Fig. 3. The effective area illustrated in Fig. 11 is expressed as follows:

$$A_\alpha(d) \equiv \mathrm{Min}[L_T(D_{\mathrm{TC}} + 2\alpha + d), L_T(D_T + d)] \tag{3}$$

This new effective area definition considers the dynamic fracture that was discussed previously in this paper. In the case that $(D_{\mathrm{TC}} + 2\alpha) > D_T$, the space debris does not collide with the tether. In this case, it is reasonable that $A_\alpha(d) = L_T(D_T + d)$. In Fig. 11, we find that

$$D_{\mathrm{TC}} + 2\alpha + 2x = D_T \tag{4}$$

The new effective area can thus be rewritten as

$$A_\alpha(d) \equiv \mathrm{Min}\left[L_T\left(\frac{1 + \gamma \mathrm{FS}}{1 + \gamma} D_{\mathrm{TC}} + d\right), L_T(D_T + d)\right] \tag{5}$$

When $\gamma = 0$ (no fracture progress), Eq. (5) turns to Eq. (2).

The amount of debris that passes within the effective cross-sectional area per year dictates the fatal impact rate R. The fatal impact rate for a tether orbiting at a certain altitude, R, is obtained by integrating the product of the effective cross-sectional area $A_\alpha(d)$ and the differential debris flux $\mathrm{d}\varphi(d)$ from d_m to ∞ with respect to the debris diameter d. The subscript α refers to the fracture progress. Thus,

$$R \equiv \int_{d_m}^{\infty} A_\alpha(d)\, \mathrm{d}\varphi(d) \tag{6}$$

6

The debris flux is determined using the ORDEM 2000 model [32] provided by NASA. Figure 12 shows an example of debris flux of the OREDM 2000, which will be used in the next section. The debris flux

Table 1 Results of hypervelocity impact experiment

Tether distance	Overlap distance	Tether diameter	Residual distance
22.5 mm	2.5 mm	10 mm	5.3 mm

Table 2 Comparison of experimental and calculated residual distances

Experiment	Calculation	Error
5.3 mm	5.2 mm	1.9%

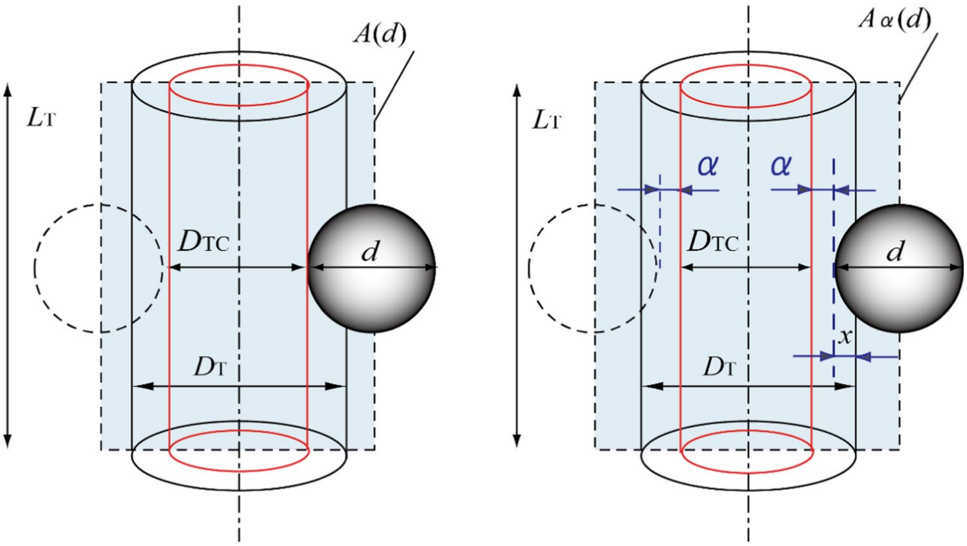

Fig. 11 Effective cross-sectional area (left: conventional approach, right: proposed approach).

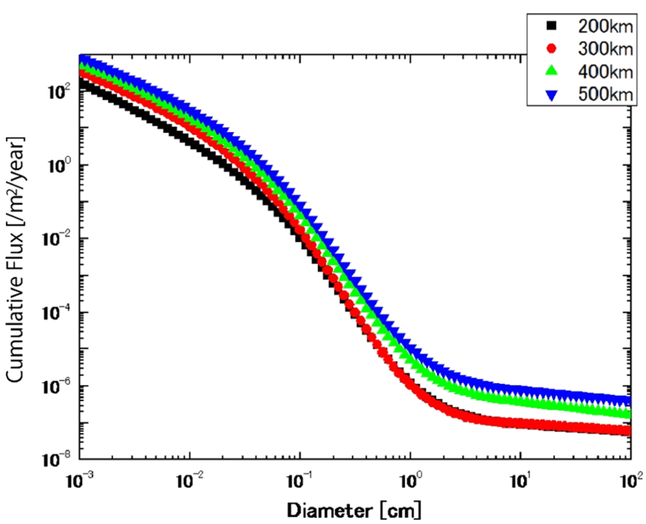

Fig. 12 Debris flux determined from ORDEM model provided by NASA.

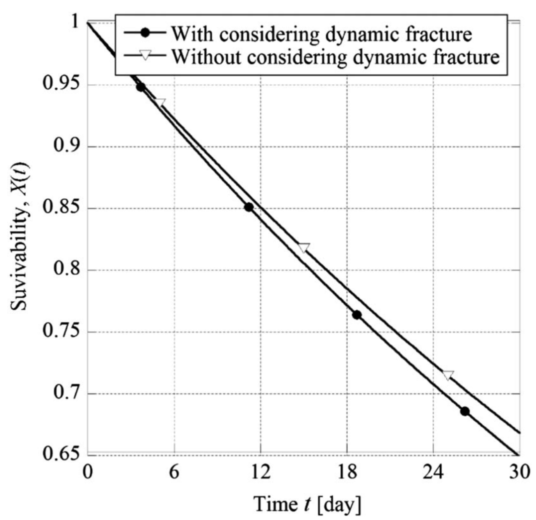

Fig. 13 Survivability of EDA in low Earth orbit.

is a function of the debris tether and the orbital altitude. The survival probability [8,17–19] of a tether at t years, $X(t)$, is calculated as follows:

$$X(t) = X(0)\exp(-Rt) \tag{7}$$

where $X(0)$ is the initial survival probability at $t = 0$.

VI. Survivability of Electrodynamic Tether in Low Earth Orbit

This section discusses a mission scenario of EDT systems to see the effect on the survivability that is described by the new formulation shown in Eq. (5). The scenario presented here is the same one that Khan and Sanmartin [20] discussed. In the following calculation, we used $\alpha = 0.253D_T$ and $\gamma = 2.98$, based on the results of the SPH simulations and impact experiments. We compared the predicted survivability obtained using our approach and that obtained using the

Table 3 Fatal impact rates per a year at an orbit at 800 km altitude

With considering dynamic fracture	Without considering dynamic fracture	Reference value [20]
5.257	4.905	4.884

conventional approach. The tether has a diameter of 1 mm and a length of 1000 m. The EDT is assumed to stay at an altitude of 800 km for a full year (1 January 2000 through 31 December 2000). The inclination of the orbit is 28.5 deg. Table 3 shows fatal impact rates per a year and 1000 m, R, for two cases (with and without considering the dynamic fracture) and reference value [20]. To compare the fatal impact rates on the same condition in Table 3, we followed the formulation of d_m that is provided in [20]. Then, in the calculation, we set $d_m = 1/3D_T$. The determination of d_m is explained in [20]. The fatal impact rate determined by considering the dynamic fracture is calculated by Eqs. (5, 6) and is 5.620. The fatal impact rate without considering the dynamic fracture is calculated by Eqs. (2, 6) and is 4.905. This number is slightly different from the reference value, 4.884. This is because the data precision of debris flux is a bit uncertain, whereas the value of debris flux in is read in the figure data that the ORDEM 2000 software provides. Because the fracture progress provides wider collision area of the tether, the risk of debris collision will definitely increase. Accordingly, it is reasonable that the fatal impact rate by considering the dynamic fracture is larger than that without considering the dynamic fracture. The conventional approach is proved to underestimate the risk of debris collision. Figure 13 shows the survivability $X(t)$ for the two approaches for a tether. The probability of survival predicted using our approach is lower than that predicted using the conventional approach. In other words, the conventional approach overestimates the survival probability of the tether. Consideration of the fracture progress provides valuable insights into the consequences of a collision between the tether and space debris and yields a different estimate of the survivability. The conventional approach to predicting the survivability of an EDT can be considered to yield overestimates. We concluded from these comparisons that future EDT mission designs should consider the dynamic fracture progress described in this paper.

VII. Conclusions

This study examines the phenomenon of dynamic fracture of a tether after a hypervelocity impact with space debris for predicting the survivability of an EDT. The tether can collide with small-sized space debris and be severed. The success of an EDT mission to remove uncontrollable satellites from LEOs depends greatly on the dynamic fracture progress of the EDT as a result of a collision with debris. This dynamic fracture progress has not been considered in
7 previous studies of EDT systems.

The phenomenon of fracture of tethers as a result of collision with small-sized debris was analyzed using SPH simulation. The results of the numerical simulation indicated that the fracture area of the tether is greater than that considered in conventional approaches to analyze EDT systems.

Hypervelocity impact experiments were also carried out to simulate collision of tethers with small-sized space debris. A method was developed to distinguish between the debris path area and the fracture area in the hypervelocity impact experiments. The results of the impact experiments confirmed that the fracture area of the tether is larger than the path area of the debris. These experimental results indicate that the fracture area will progress after collision of the tether with space debris.

Based on these results, a more accurate way to estimate the survival probability of an EDT system was developed that considers the distance of the fracture progress after collision with space debris. It was confirmed that the survivability estimate obtained using the proposed approach is lower than that obtained using the conventional approach. The superiority of the present approach is expected to contribute to the success of EDT missions in removing space debris and thus help accelerate space development. Furthermore, the proposed approach can theoretically be applied to the safety evaluation of a space elevator having thin and long tethers.

Acknowledgments

The experiments described in this paper were conducted and
8 supported by the Shock Wave Research Facilities, Institute of Fluid Science, at Tohoku University. This study was supported by ISAS/JAXA as a collaborative program with the Space Plasma Laboratory.

9

References

[1] Pelton, N. J., *Space Debris and Other Threats from Outer Space*,
10 Springer Briefs in Space Development, Springer-Verlag, New York, 2013.

[2] Vaibhav, L. D., and Ugur, G., *Introduction to Space Debris: Challenges and Removal Techniques*, Lambert Academic, 2013.

[3] Cosmo, M. L., and Lorenzini, E. C., *Tethers in Space Handbook*, 3rd ed., Smithsonian Astrophysical Observatory, Cambridge, MA, 1997.

[4] Iess, L., Bruno, C., Ulivieri, C., and Vannaroni, G., "Satellite De-Orbiting by Means of Electrodynamic Tethers, Part 2: System Configuration and Performance," *Acta Astronautica*, Vol. 50, No. 7, 2002, pp. 407–416. doi:10.1016/S0094-5765(01)00181-3

[5] Ishige, Y., Kawamoto, S., and Kibe, S., "Study on Electro Dynamic Tether System for Space Debris Removal," *Acta Astronautica*, Vol. 55, No. 11, 2004, pp. 917–929. doi:10.1016/j.actaastro.2004.04.015

[6] Anselmo, L., and Pardini, C., "The Survivability of Space Tether Systems in Orbit around the Earth," *Acta Astronautica*, Vol. 56, No. 3, 2005, pp. 391–396. doi:10.1016/j.actaastro.2004.05.067

[7] Liou, J. C., and Johnson, N. L. A., "A Sensitivity Study of the Effectiveness of Active Debris Removal in LEO," *Acta Astronautica*, Vol. 64, Nos. 2–3, 2009, pp. 236–243. doi:10.1016/j.actaastro.2008.07.009

[8] Pardini, C., Hanada, T., and Krisko, P. H., "Benefits and Risks of Using Electrodynamic Tethers to De-Orbit Spacecraft," *Acta Astronautica*, Vol. 64, Nos. 5–6, 2009, pp. 571–588. doi:10.1016/j.actaastro.2008.10.007

[9] Forward, R. L., and Hoyt, R. P., "Terminator Tether™: A Spacecraft Deorbit Device," *Journal of Spacecraft and Rockets*, Vol. 37, No. 2, 2000, pp. 187–196. doi:10.2514/2.3565

[10] Van der Heide, E. J., and Kruijff, M., "Tethers and Debris Mitigation," *Acta Astronautica*, Vol. 48, Nos. 5–12, 2001, pp. 503–516.
doi:10.1016/S0094-5765(01)00074-1 11

[11] Bonnal, C., Ruault, J.-M., and Desjean, M.-C., "Active Debris Removal: Recent Progress and Current Trends," *Acta Astronautica*, Vol. 85, 2013, pp. 51–60. doi:10.1016/j.actaastro.2012.11.009

[12] Corsi, J., and Iess, L., "Stability and Control of Electrodynamic Tethers for De-Orbiting App1ications," *Acta Astronautica*, Vol. 48, Nos. 5–12, 2001, pp. 491–501. doi:10.1016/S0094-5765(01)00049-2

[13] Yamaigiwa, Y., Hiragi, E., and Kishimoto, T., "Dynamic Behavior of Electrodynamic Tether Deorbit System on Elliptical Orbit and Its Control by Lorentz Force," *Aerospace Science and Technology*, Vol. 9, No. 4, 2005, pp. 366–373. doi:10.1016/j.ast.2004.09.005

[14] Mantri, P., Mazzoleni, P. A., and Padgett, A. D., "Parametric Study of Deployment of Tethered Satellite Systems," *Journal of Spacecraft and Rockets*, Vol. 44, No. 2, 2007, pp. 412–423. doi:10.2514/1.22955

[15] Jung, W., Mazzoleni, P. A., and Chung, J., "Dynamic Analysis of a Tethered Satellite System with a Moving Mass," *Nonlinear Dynamics*, Vol. 75, Nos. 1–2, 2014, pp. 267–281. doi:10.1007/s11071-013-1064-8

[16] Patera, R. P., "Method for Calculating Collision Probability Between a Satellite and a Space Tether," *Journal of Guidance, Control, and Dynamics*, Vol. 25, No. 5, 2002, pp. 940–945. doi:10.2514/2.4967

[17] Gittins, G. L., Swinerd, G. G., Lewis, H. G., and Williams, D. N., "A Study of Debris Impact Collision Probabilities to Space Tethers,"
Advances in Space Research, Vol. 34, No. 5, 2004, pp. 1080–1084. 12
doi:10.1016/j.asr.2003.01.013

[18] Pardini, C., Anselmo, L., Hanada, T., and Hirayama, H., "Assessing the Vulnerability to Debris Impacts of Electro Dynamic Tethers During Typical De-Orbiting Missions," *Proceedings of the 4th European Conf. on Space Debris*, European Space Agency SP-587, Paris, 2005.

[19] Pardini, C., Hanada, T., Krisko, P. H., Anselmo, L., and Hirayama, H., "Are De-Orbiting Missions Possible Using Electrodynamic Tethers? Task Review from the Space Debris Perspective," *Acta Astronautica*, Vol. 60, Nos. 10–11, 2007, pp. 916–929. doi:10.1016/j.actaastro.2006.11.001

[20] Khan, B. S., and Sanmartin, R. J., "Survival Probability of Round and Tape Tethers Against Debris Impact," *Journal of Spacecraft and Rockets*, Vol. 50, No. 3, 2013, pp. 603–608.
doi:10.2514/1.A32383 13

[21] Simon, C. G., Hunter, J. L., Griffis, D. P., Misra, V., Ricks, D. A., Wortman, J. J., and Brownlee, D. E., "Elemental Analyses of Hypervelocity Microparticle Impact Sites on Interplanetary Dust Experiment Sensor Surfaces," *Proceedings of the 2nd Post-Retrieval Symposium*, NASA Langley Research Center Rept. N93-29354, Vol. 2, 1993, pp. 677–692.

[22] Kawai, N., Tsurui, K., Hasegawa, S., and Sato, E., "Single Microparticle Launching Method Using Two-Stage Light-Gas Gun for Simulating Hypervelocity Impacts of Micrometeoroids and Space Debris," *Review of Scientific Instruments*, Vol. 81, No. 11, 2010, Paper 115105. doi:10.1063/1.3498896

[23] Hörtz, F., Cintala, M. J., Bernhard, R. P., and See, T. H., "Experimental Impacts into Teflon Targets and LDEF Thermal Blankets," *Proceedings of the 25th Lunar and Planetary Science Conf.*, Part 2, Houston, TX, 1994, pp. 567–568.

[24] Sabath, D., and Paul, K. G., "Hypervelocity Impact Experiments on Non-Conductive Tether Materials," *Advances in Space Research*, Vol. 20, No. 8, 1997, pp. 1433–1436. doi:10.1016/S0273-1177(97)00410-9

[25] Francesconi, A., Giacomuzzo, C., Branz, F., and Lorenzini, E. C., "Survivability to Hypervelocity Impacts of Electrodynamic Tape Tethers for Deorbiting Spacecraft in LEO," *Proceedings of the 6th European Conf. on Space Debris*, European Space Agency SP-723, Paris, 2013.

14

[26] Randles, P. W., and Libersky, L. D., “Smoothed Particle Hydrodynamics: Some Recent Improvements and Applications,” *Computer Methods in Applied Mechanics and Engineering*, Vol. 139, Nos. 1–4, 1996, pp. 375–408.
doi:10.1016/S0045-7825(96)01090-0

[27] Beltrami, P., “Comparison of Debris Flux Models,” Final Rept. of IADC Action Item 19.2, Document No. IADC-05-03, 2005.

[28] Pardini, C., Hanada, T., and Krisko, P. H., “Potential Benefits and Risks of Using Electrodynamic Tethers for End-of-Life De-Orbit of LEO Spacecraft,” Final Rept. of IADC Action Item 19.1, Document No. IADC-06-02, 2006.

[29] Ohtani, K., Numata, D., Kikuchi, T., Sun, M., Takayama, K., and Togami, K., “A Study of Hypervelocity Impact on Cryogenic Materials,” *International Journal of Impact Engineering*, Vol. 33, Nos. 1–12, 2006, pp. 555–565.
doi:10.1016/j.ijimpeng.2006.09.025

[30] Yanagida, A., Kawamoto, S., Higashide, M., Hasegawa, S., and Toda, S., “Study of Hypervelocity Impact on Electrodynamic Tether for Tether Lifetime Evaluation,” *Proceedings of the 61st International Astronautical Congress*, IAC-10_A6_3_8_x9026, 2010.

[31] Khan, B. S., and Sanmartin, R. J., “Analysis of Tape Tether Survival in LEO Against Orbital Debris,” *Advances in Space Research*, Vol. 53, No. 9, 2014, pp. 1370–1376.
doi:10.1016/j.asr.2014.02.008

[32] Liou, J. C., Matney, M. J., Anz-Meador, P. D., Kessler, D., Jansen, M., and Theall, J. R., “The New NASA Orbital Debris Engineering Model ORDEM-2000,” NASA TP-2002-210780, Johnson Space Center, Houston, TX, 2002.

Dr. A. Ketsdever
Associate Editor